

REVISED VERSION

1 Effect of magnesium addition on the cell structure of foams produced from 2 re-melted aluminium alloy scrap

3 G. S. Vinod-Kumar^{1,4*}, K. Heim^{1,2}, J. Jerry⁴, F. Garcia-Moreno^{1,2}, A. R. Kennedy³, J. Banhart^{1,2}

4 ¹Technische Universität Berlin, Hardenbergstraße 36, 10623 Berlin, Germany

5 ²Helmholtz-Zentrum Berlin für Materialien und Energie, Hahn Meitner Platz, 14109 Berlin, Germany

6 ³Division of Manufacturing, University of Nottingham, Nottingham, NG2 7RD, UK,

7 ⁴SRM Research Institute, SRM University, Kattankulathur, 603203, India

8 Abstract

9 Closed-cell foams were produced from re-melted aluminium alloy scrap that contained
10 0.13 wt.% Mg magnesium in the as-received state and higher levels after adding 1, 2 or
11 5 wt.% Mg. The excess Mg gave rise to the fragmentation of long oxide filaments present in
12 the scrap alloy into smaller filaments and improved its distribution and wetting by the Al ma-
13 trix. Foaming the re-melted scrap alloy containing 1,2 and 5 wt.% Mg excess showed stabil-
14 ity and good expansion in comparison to the scrap alloy containing 0.13 wt.% Mg only, but
15 the cells became non-equiaxed when the Mg concentration was high (≥ 2 wt.% excess) due to
16 cell wall rupture during solidification. Compressibility and energy absorption behaviour were
17 studied for scrap alloy foams containing 1 wt.% Mg excess, which is the optimum level to
18 obtain good expansion, stability and uniform cell size. Foams with densities in the range of
19 0.2-0.4 g·cm⁻³ produced by holding at the foaming temperature for different times were used
20 for the investigation. A uniform cell structure led to flatter stress plateaus, higher energy ab-
21 sorption efficiencies and reduced "knockdown" in strength compared with commercial foams
22 made by gas bubbling. The mechanical performance found is comparable to that of commer-
23 cial foams made by a similar method but the expected costs are lower.

*Corresponding Author: Dr. G. S. Vinod Kumar, email id: vinodnarasimha@gmail.com

24 **Keywords**

25 Scrap aluminium alloy, Closed cell Al foams, oxide bi-films, $MgAl_2O_4$ (spinal), compressive
26 strength

27 **1. Introduction**

28 Closed-cell aluminum alloy foams produced through the liquid metal route are potentially
29 cheaper in comparison to foams produced using metal powders because of the lower number
30 of processing steps[1-2]. Liquid metal foaming requires ceramic or intermetallic particles for
31 foam stabilization [3-5].Ceramic particles such as SiC, Al_2O_3 , TiB_2 , TiC[6] and also
32 $MgAl_2O_4$ [7] have been found to be effective stabilizing agents for aluminum foams but the
33 introduction of these particles into the matrix requires additional processing steps. There is a
34 school of thought that oxide bi-films which get entrapped during ingot casting will also acts
35 as stabilisation agent for foams[6, 8].

36 Attempts have been made to utilise the foam-stabilizing properties of oxide bi-films by using
37 scrap aluminium alloys produced by melting swarfs (machining chips and turnings of auto-
38 motive castings) as a foamable precursor. By re-melting these swarfs the thick oxide skins
39 contained are introduced into the alloy as oxide films. Ha et al. reported that these oxide films
40 enhance viscosity of the melt and aid in foaming [9]. Haesche et al. have utilised thixo cast-
41 ing to produce foamable precursors from $AlSi9Cu3$ or $AlMg4.5Mn$ alloy chips by using-
42 $CaCO_3$ or $CaMg(CO_3)_2$ as a blowing agent[10]. However, in all previous studies it was re-
43 ported that the observed cell morphology of scrap aluminium alloy foam was distorted due to
44 the poor distribution of inherent oxides in the matrix. Using scrap alloys for foaming finds
45 potential due to their low cost in comparison to expensive particle-reinforced metal matrix
46 composites produced by ex-situ or in-situ methods. The authors have demonstrated in previ-
47 ous studies[11-12]that re-melted scrap aluminium alloy foams with optimum expansion and
48 stability can be made by adding Mg while melting the swarfs (machining chips or turnings of

49 LM26 alloy castings) and holding them in the liquid state during which the oxides are dis-
50 persed. To enable the reaction, the oxide concentration in the scrap was increased by heat
51 treating the swarfs at 500 °C for several hours before melting. 1 or 2 wt.% Mg was added and
52 this Mg reacts with the oxides to form $MgAl_2O_4$ (spinel) and MgO as reaction products. This
53 promotes good wetting of oxides and distributes them uniformly in the Al matrix.

54 In the work presented here, the cell structure and cell size distribution of re-melted Al scrap
55 alloy foams containing various concentrations of Mg (0.13 wt.% as-received, and 1, 2 and 5
56 wt.% in excess to this level) and foamed at various holding time was investigated. The aim of
57 this study was to understand to which extent the inherent oxides filaments undergo fragmen-
58 tation and how much $MgAl_2O_4$ and MgO is formed when Mg is added at increased levels.
59 The results are correlated to the expansion, stability, cell structure and cell size distribution of
60 the foams produced. The main difference between the scrap alloy used in the present and pre-
61 vious work [11-12] is the oxide concentration, which is less in the present work since no heat
62 treatment was carried out for the swarfs before melting.

63 The prospects of using re-melted Al scrap alloy foams in structural applications have to be
64 evaluated even though they show a promising foaming behaviour. The base alloy of the
65 swarfs, LM26, exhibits very low ductility and the presence of oxides further decreases ductil-
66 ity and deteriorates the mechanical properties of the foam. Therefore, the compressibility and
67 the energy absorption behaviour of foams of various densities displaying good cell structure
68 and distribution were studied. Their performance is compared to foams made by commercial-
69 ly available liquid routes, also known as Cymat and Alporas foams.

70 **2. Experimental Procedure**

71 The scrap used in the present study was received as mm-sized swarfs (machining chips and
72 turnings) of LM26 (Al-10 wt.%Si-3 wt.% Cu) alloy, which is commonly used for making
73 automotive castings. The morphology of the chips and the approximate composition as meas-

74 ured by optical emission spectroscopy (OES) is given in [table 1](#). The machining chips already
75 contain 0.13 wt.% of Mg in the as-received state. The material was first heated to 673 K
76 (400 °C) to remove residual oil and cutting lubricants. Then it was directly converted into
77 ingots by melting in a graphite crucible at 1023 K (750 °C). No additional heat treatment was
78 carried out as done in previous studies where the oxide content in the swarfs was increased
79 [11-12]. During melting, the chips were fused by vigorous intermittent stirring for 30 min.
80 Magnesium was admixed in excess to 0.13 wt.% (base alloy concentration) at various levels
81 (1, 2 and 5 wt.%) by using a Al-25 wt.% Mg master alloy. After this, the melt was kept iso-
82 thermally at 1023 K (750 °C) for 4 h for conditioning (reaction). The conditioned melt was
83 again stirred and cast into a steel mould. X-ray diffraction for phase analysis of the scrap al-
84 loys was performed using Cu-K α radiation. The re-melted scrap alloys (and cross sections of
85 foams) were metallographically polished and electro-polished using a mixture of orthophos-
86 phoric acid, ethanol and water as the electrolyte. The polished samples were observed using a
87 high-resolution scanning electron microscope (HRSEM). Elemental analysis was done using
88 energy dispersive X-ray spectroscopy (EDX).

89 Foaming was performed by melting 40 g of each alloy in an alumina crucible in a re-
90 sistive heating furnace at 973 K (700 °C). After the melt had reached the desired temperature,
91 1.6 wt.% of as-received TiH₂ powder was admixed to the melt using a graphite stirrer rotating
92 at 600 rpm for 80 s. After mixing, the melt was held isothermally inside the furnace for dif-
93 ferent holding times, namely 100 s, 140 s and 180 s, during which it was allowed to foam.
94 After this, the sample was taken out and allowed to solidify in resting air. X-ray tomography
95 of the foams was performed by rotating them through 360° in steps of 1° while acquiring X-ray
96 radiographic images after each step. Three-dimensional (3D) reconstruction of the data was car-
97 ried out using the commercial software ‘Octopus’. After reconstruction, the commercial software
98 ‘VGStudioMax 1.2.1’ was used to extract 2D and 3D sections of the foam. The 2D cell area dis-

99 tribution and circularity for selected foams was calculated by analyzing the reconstructed tomo-
100 graphic slices taken from the central part of the foams. This analysis was performed by using the
101 software 'Image J 1.35j'.

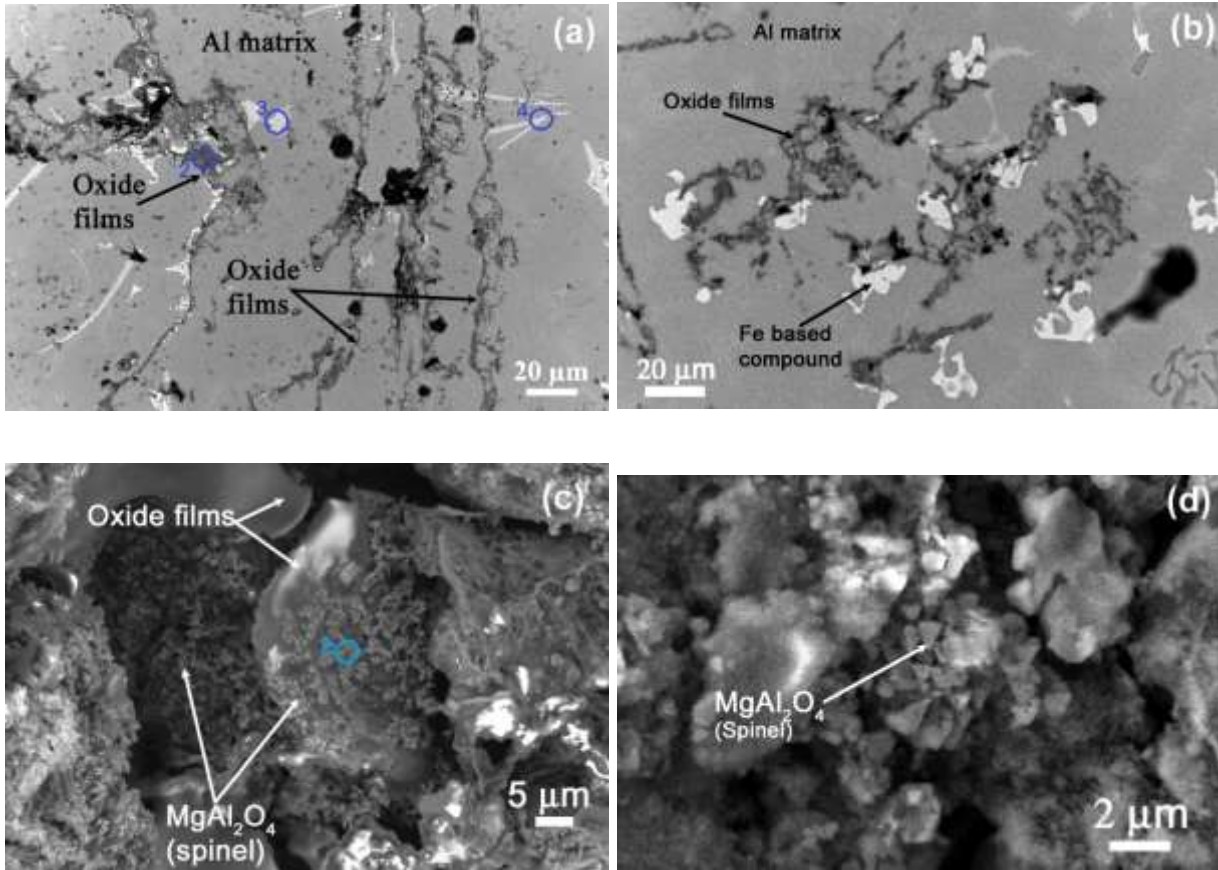
102 For compression tests, foams were made from the alloy containing a Mg excess of 1 wt.%
103 and applying holding times of either 100 s or 140 s. Samples of $\sim(25 \times 25 \times 25)$ mm³ size were
104 sliced by electro-discharge machining. Compression testing was performed at a rate of
105 2 mm min⁻¹. Mechanical testing and data analysis were conducted according to "ISO
106 13314:2011(E)" standard.

107

108 **3. Results**

109 Figures 1a and b show SEM photomicrographs of re-melted scrap alloy in the as-received
110 condition (containing 0.13wt.% of Mg) and in the alloy with 1wt.% excess Mg addition. The
111 longer aluminium oxide filaments seen in the aluminium matrix (Fig. 1a) containing only
112 0.13 wt.% of Mg get fragmented into smaller oxide films after adding 1 wt.% Mg (Fig. 1b).
113 The alloy also shows Fe- and Cu-based intermetallic compounds in the matrix. A closer look
114 at the microstructure (Fig. 1c,d) of the re-melted scrap alloy containing 1wt.% Mg shows that
115 the surface of the fragmented oxide films is covered by fine MgAl₂O₄ (spinel) particles of less
116 than 2 μm size.

117



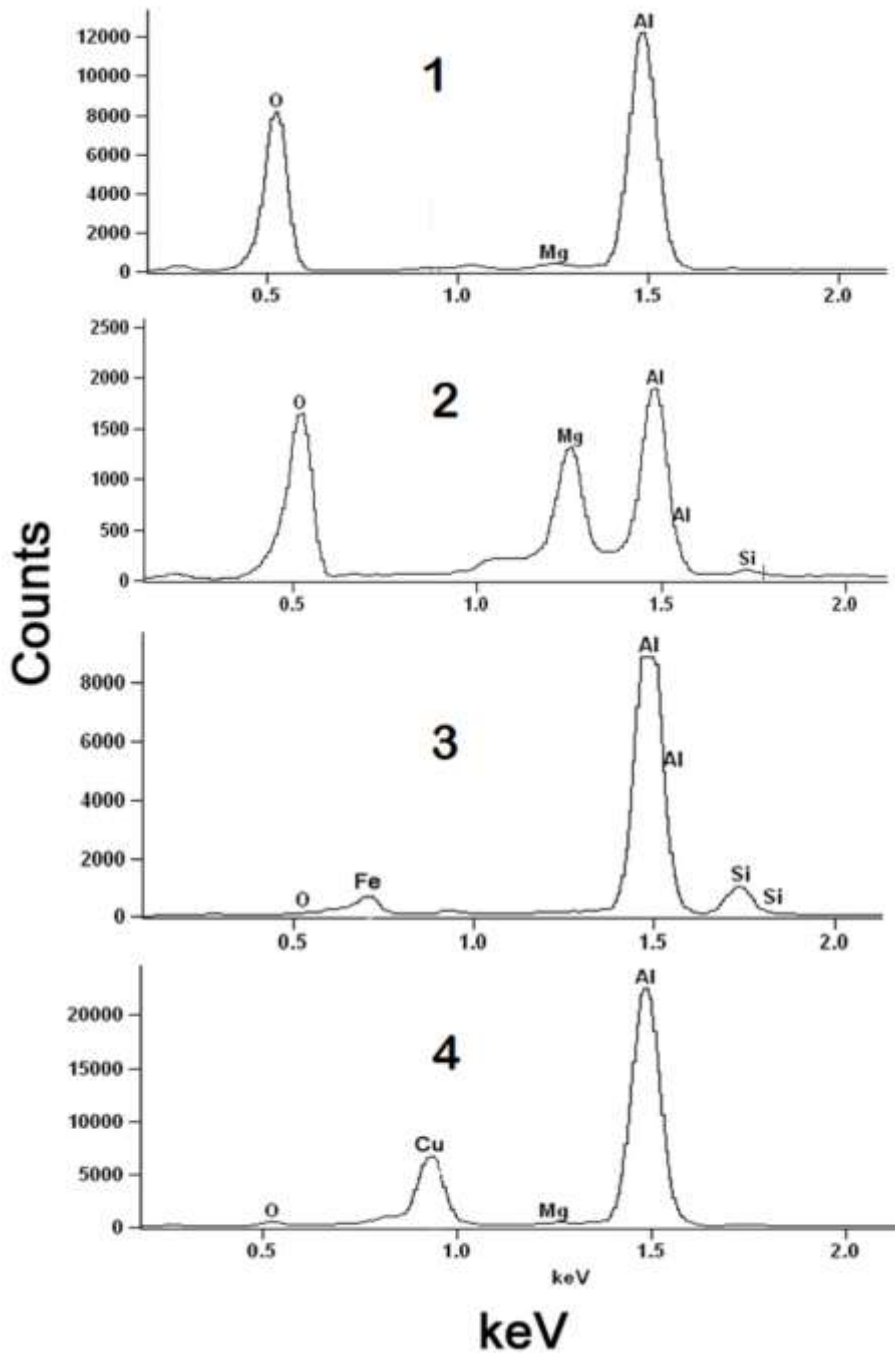
118

119

120 **Fig.1** SEM micrographs of re-melted aluminium scrap alloy. (a) As received (0.13 wt.%Mg),
 121 (b) with 1 wt.% Mg excess, (c) MgAl₂O₄ particles on the surface of an Al oxide film,
 122 (d) octahedral morphology of MgAl₂O₄ spinel particles.

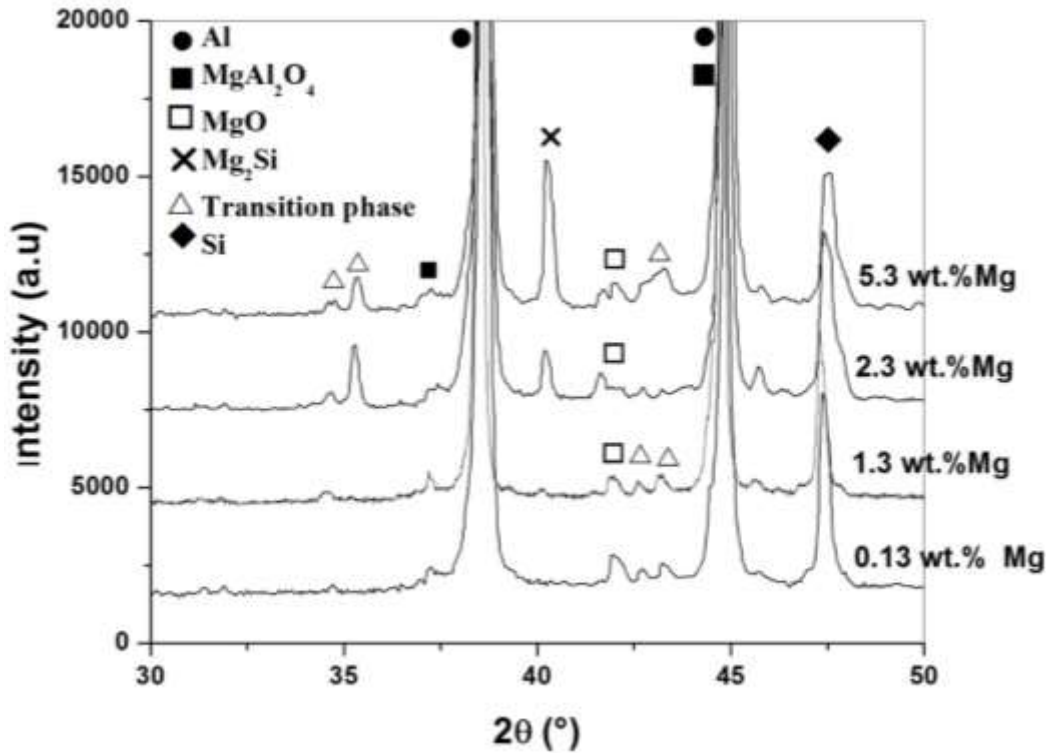
123 The EDX stacked spectrums (Fig.2) taken at different particles (one spectrum for each parti-
 124 cle) confirms the presence of Al₂O₃, MgAl₂O₄ and other Fe- and Cu-based intermetallic com-
 125 pounds in the aluminium matrix. The regions in which EDX spectra were taken are encircled
 126 in the SEM pictures (Fig.1a,c). The X-ray diffraction patterns (Fig. 3) of the re-melted alu-
 127 minium scrap alloys containing various amounts of Mg (0, 1, 2 and 5 wt.% in excess to the
 128 0.13 wt.% in the as-received material) point at the presence of MgAl₂O₄, MgO, Mg₂Si and
 129 small amounts of other transition phases. The XRD spectra show that addition of more Mg
 130 does not increase the amount of MgAl₂O₄ or MgO in the alloys as seen by the peak intensities
 131 of the spectra. Their formation is rather governed by the amount of oxygen available in an

132 alloy, which is independent of Mg content. However, increasing the Mg content does increase
133 the level of Mg₂Si formation.



134
135 Fig.2 Energy dispersive spectrum (EDX) of (1) aluminium oxide, (2) MgAl₂O₄, (3) Fe-based
136 and (4) Cu-based intermetallics present in the alloy. The regions in which the EDX
137 spectra were taken are encircled in the SEM micrographs of Figure 1.

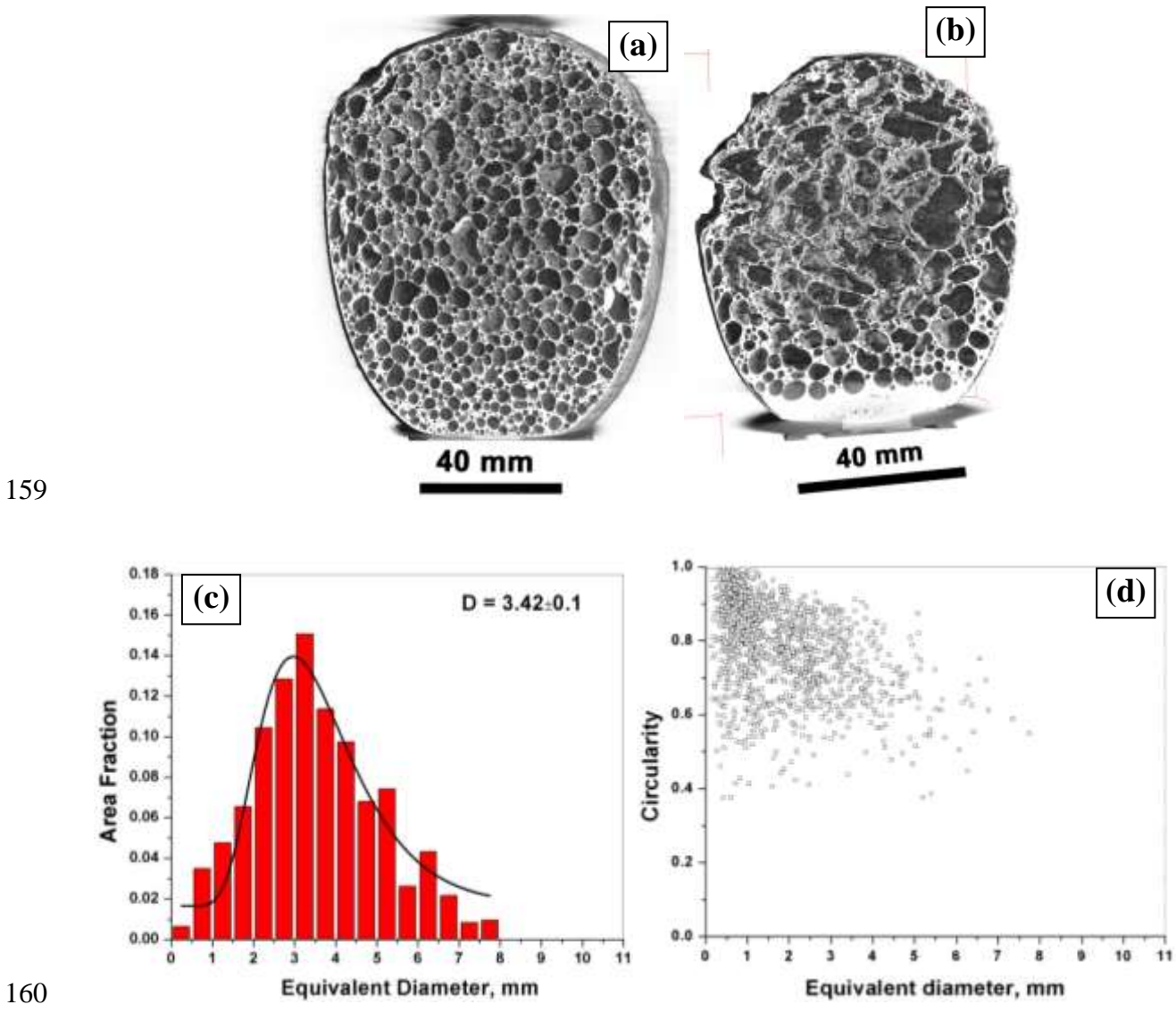
138



139
 140 **Fig.3** XRD plots of re-melted aluminium scrap alloy with various Mg concentrations.

141 Figure 4 a,b shows X-ray tomographic reconstructions of longitudinal cross sections of foams
 142 produced from re-melted scrap alloys containing 0.13 wt.% Mg. The foams were produced at
 143 973 K (700 °C) and held for 100 s (Fig.4a) or 140 s (Fig.4b) and were solidified by air cool-
 144 ing. The foam showed good expansion after 100 s of holding at the foaming temperature and
 145 its macrostructure exhibits an equiaxed cell structure and uniform cell size distribution
 146 throughout the cross section. No defects such cell wall rupture, deformed cells or drainage are
 147 observed. Upon holding for 140 s the foam started to collapse. The liquid sump at the bottom
 148 of the foam indicates drainage (Fig. 4b).The 2Dcell size distribution of the foam obtained
 149 after 100 s of holding is given in Fig. 4c.The analysis is based on the area fraction, which is
 150 defined as the area contribution of a cell size class related to the total area of all the cells
 151 [13].The mean cell size D as provided by log-normal fitting of the distributions is
 152 3.42 ± 0.1 mm. The cells in the foam held for 140 s are full of defects and irregular and there-
 153 fore no reliable analysis could be performed.

154 The 2D cell circularity of the foam obtained after 100 s of holding shows (Fig. 4d) that most
 155 of the cells are close to circularity, indicating that they are of equiaxed (polyhedral) shape.
 156 Here, the circularity C of a cell is defined as $4\pi A/P^2$, where A and P are the area and perime-
 157 ter of the cell, respectively. If C approaches 1, a cell resembles a circle. The details of the
 158 analysis are reported in Ref. [13].



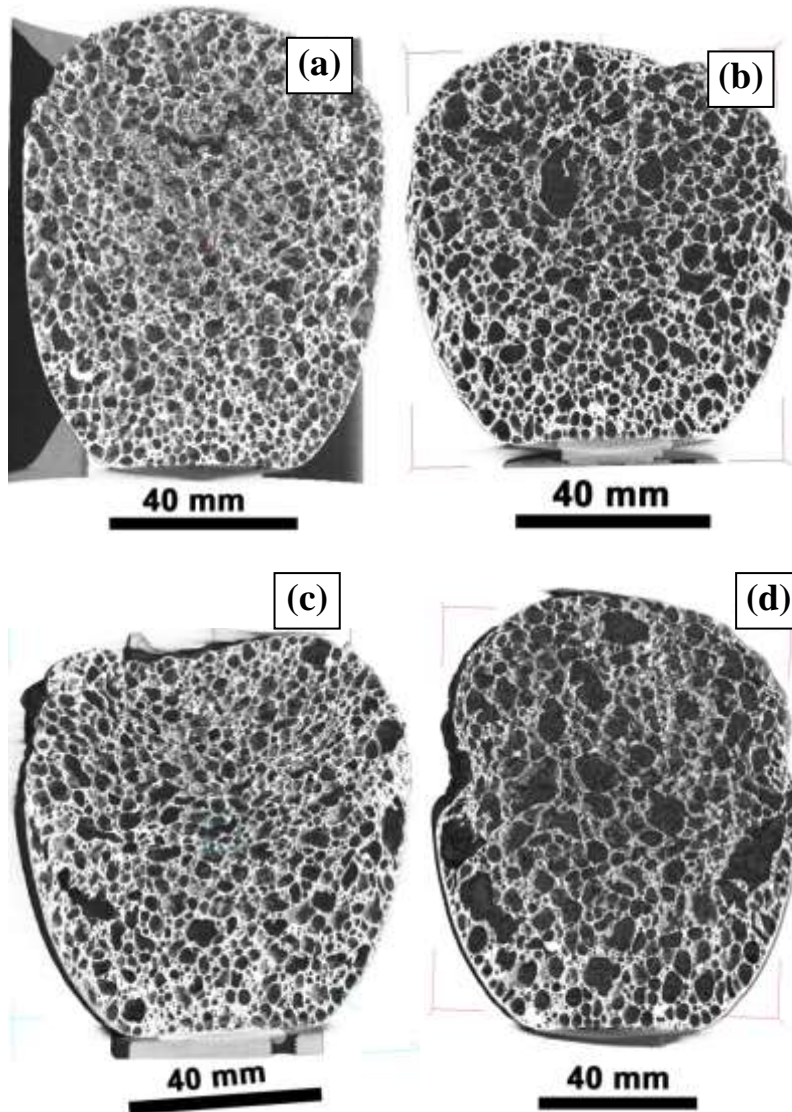
160
 161 **Fig.4** X-ray tomographic reconstructions of longitudinal cross sections of foams made from
 162 scrap alloy containing 0.13 wt.% Mg and produced by uninterrupted foaming in an
 163 alumina crucible at 973 K (700 °C) for (a) 100 s (b) 140 s. (c) 2D cell size distribution
 164 and (d) Circularity vs. equivalent diameter of the cells for the foam held for 100 s.

165 Figures 5 a - c shows 3D X-ray tomographic reconstructions of longitudinal cross sections of
166 foams produced from re-melted scrap alloys containing 1, 2 and 5 wt.% Mg addition. The
167 foams were produced at 973 K (700 °C) and held for 140 s before solidification. Figure 5 d
168 shows the macrostructure of the foam containing 5 wt.% Mg, which was held for 180 s. For
169 100 s holding time, the expansion was not complete for the foams containing 1, 2 and 5 wt.%
170 Mg addition. Delayed expansion of foam with increased Mg content was already reported in
171 Refs. [11-12]. The foam with 1 wt.% Mg addition showed good expansion and stability even
172 after 140 s of holding unlike the foam with 0.13 wt.% Mg content. The cells are finer and
173 equiaxed in shape and uniformly distributed throughout the cross section. The expansion ob-
174 served for the foams with 2 and 5 wt.% Mg is less in comparison to that of the foam contain-
175 ing 1 wt.% Mg. The cell structure of the foams with 2 and 5 wt.% Mg addition are non-
176 equiaxed in shape in comparison to 1 wt.% Mg, see below for a quantitative analysis. To wit-
177 ness expansion during further holding, the alloy containing 5 wt.% Mg excess was also held
178 at the foaming temperature for 180 s. The foam continued to expand, but the foam structure
179 exhibited many large cells of irregular shape after. No drainage was seen in any of the foams
180 containing 1, 2 and 5 wt.% Mg excess that was held for 140 s or 180 s.

181

182

183



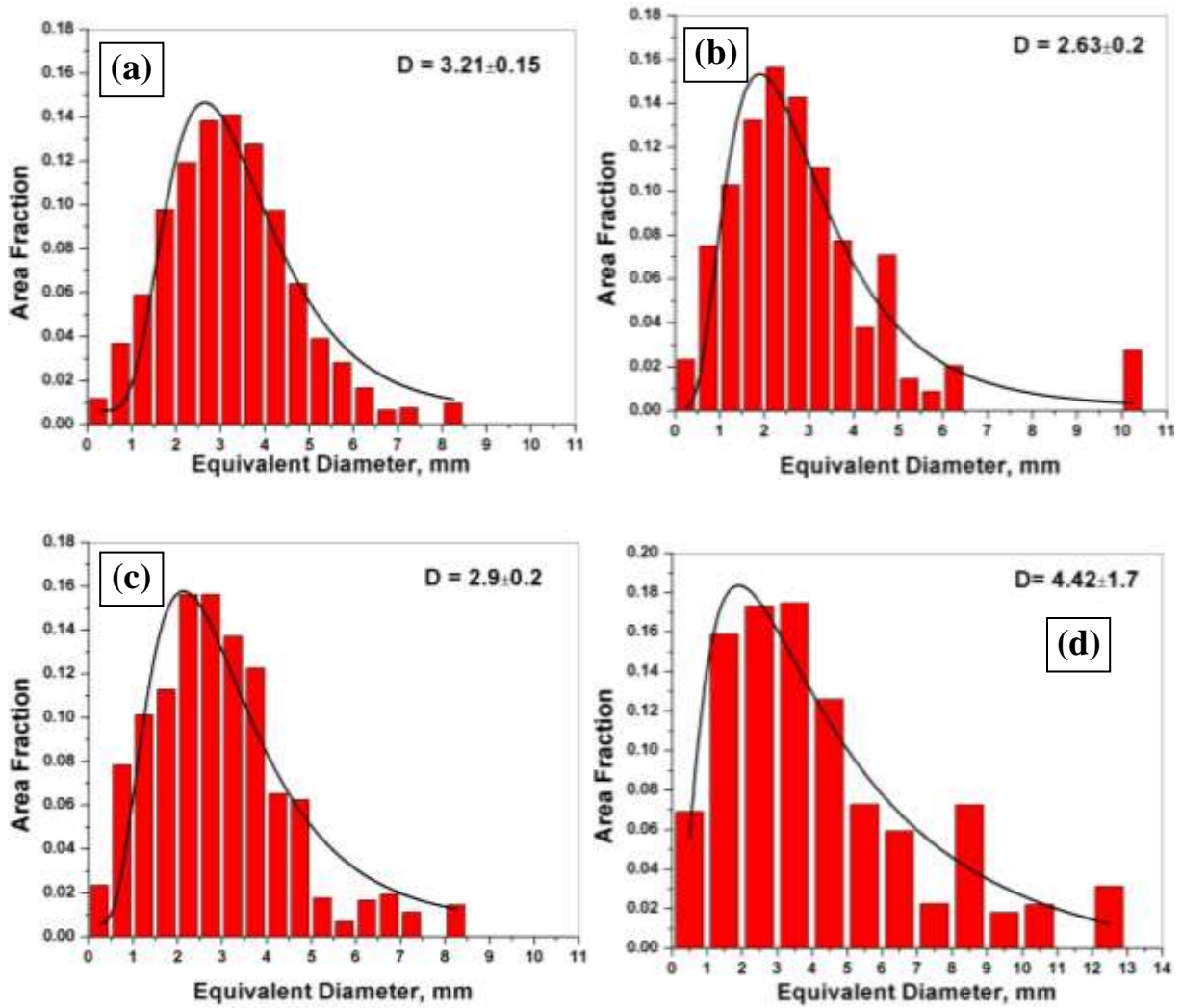
184

185

186 **Fig.5** X-ray tomographic reconstructions of longitudinal cross sections of scrap alloy foams
 187 produced by uninterrupted foaming in an alumina crucible at 973 K (700 °C) for 140 s. (a)
 188 1 wt.% Mg, (b) 2 wt.% Mg, (c) 5 wt.% Mg and (d) foam containing 5 wt.% Mg held for
 189 180 s.

190 Analysis of the 2D cell size distribution was done for the foams containing 1, 2 or 5 wt.% Mg
 191 excess that were held for 140 s, see Fig. 6 a-c. The foam with 1 wt.% Mg addition shows an
 192 uniform cell size distribution and a mean cell size D of 3.21 ± 0.15 mm. In contrast, the analy-
 193 sis reveals a non-uniform cell size distribution for the foam with 2 and 5 wt.% Mg excess
 194 with slightly lower mean cell sizes. The foam containing 5 wt.% Mg excess was held for

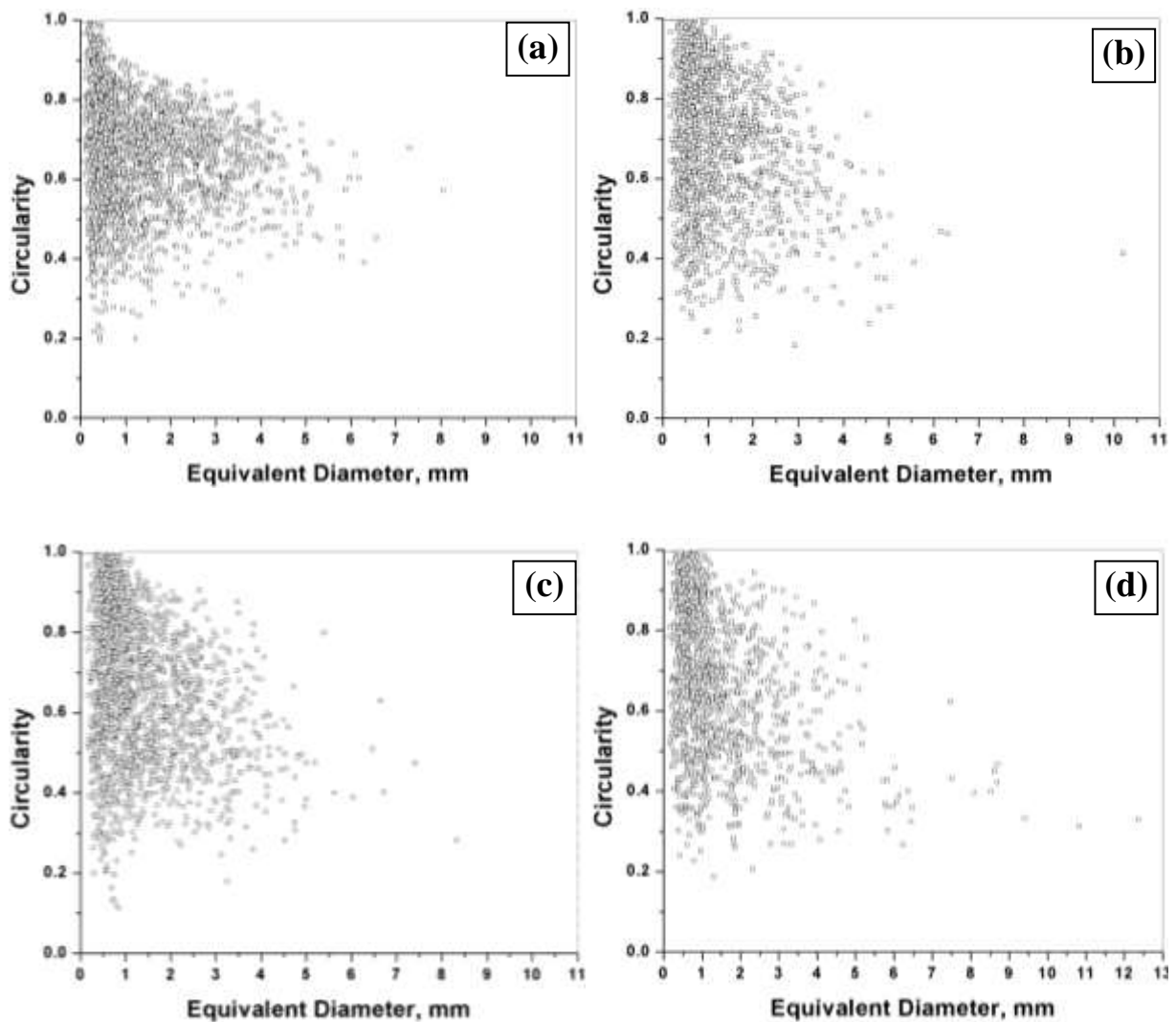
195 180 s and exhibits even larger mean cell size D , see Fig. 6d. There is no trend in the cell size
 196 distribution as a function of Mg addition, but there is a significant increase in the cell size
 197 when the time of holding of the foams is increased to 180 s.



198
 199
 200 **Fig.6** 2D cell size distributions for scrap alloy foams produced by uninterrupted foaming in
 201 an alumina crucible at 973 K (700 °C) for 140 s. (a) 1 wt.% Mg addition, (b) 2 wt.%
 202 Mg addition, (c) 5 wt.% Mg addition, (d) 5 wt.% Mg addition but 180 s holding time.

203 The 2D cell circularity analysis (Fig. 7a-c) of the foams with 1, 2 and 5 wt.% Mg excess held
 204 for 140 s shows that a large number of cells are not equiaxed and this number increases with
 205 an increase in Mg. The foam with 5 wt.% Mg excess and held for 180 s also contains non-
 206 equiaxed large cells. The cell circularity of the foam containing 0.13 wt.% Mg obtained after

207 100 s foaming (Fig.4d) is not comparable with that of the foams with 1, 2 and 5 wt.% Mg
208 excess. The former showed mostly equiaxed cells throughout the foam cross section.

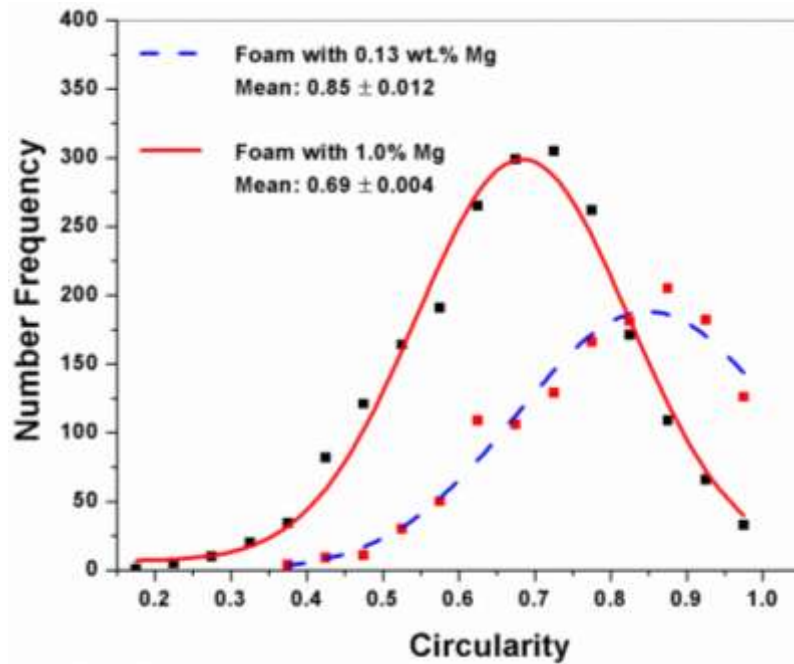


211 **Fig.7** Circularity vs. equivalent diameter of the cells in re-melted scrap alloy foams produced
212 by uninterrupted foaming in an alumina crucible at 973 K (700 °C) for 140 s. (a) to (d) corre-
213 sponding to Fig. 5.

214 Figure 8 shows the comparative plot of circularity of the foams containing 0.13wt.% Mg and
215 1 wt.% Mg. The mean circularity value of the former is 0.85 ± 0.012 while the latter is
216 0.69 ± 0.004 .

217

218



219

220 **Fig.8** Comparison of circularity of foams containing 0.13wt.% Mg (Fig. 3d) and 1 wt.% Mg

221 (Fig. 6a). The mean circularity value (Gaussian fit) of the foam containing 0.13wt.%

222 Mg is 0.85 ± 0.012 and for the foam containing 1wt.% Mg 0.69 ± 0.004 .

223 For comparison of cell structure, an X-ray tomographic reconstruction of a transverse section

224 of the foam with 0.13 wt.% Mg obtained after 100 s of holding is compared to reconstruc-

225 tions of foams containing 1, 2 or 5 wt.% Mg excess and foamed for 140 s (Fig. 9).Clearly, the

226 foams with higher Mg contents exhibit a less equiaxed cell structure and less uniform distri-

227 bution in comparison to the foam with 0.13 wt.% Mg. All the elongated cells are associated

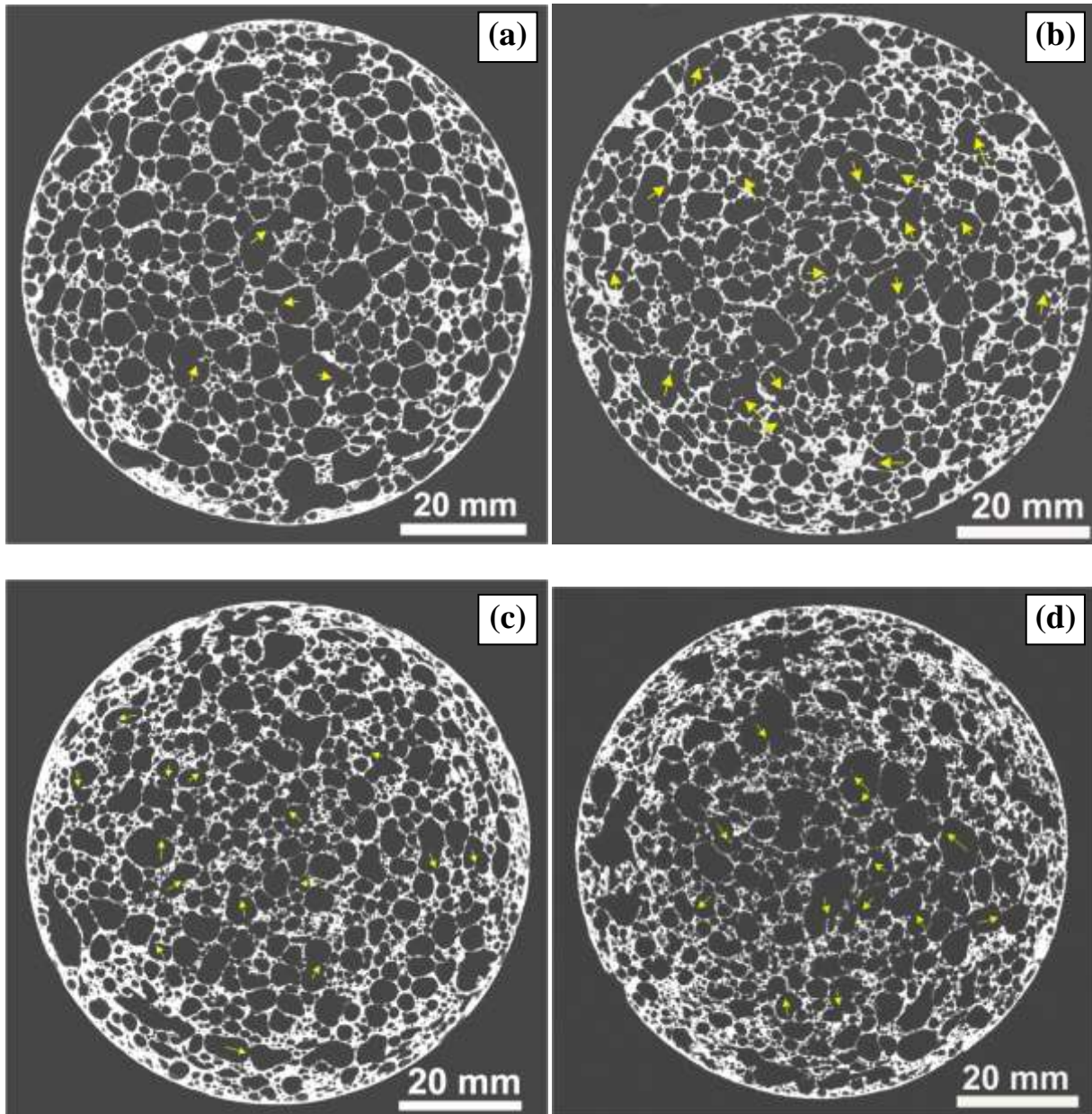
228 with remnants of broken cell walls, which indicate that cell wall rupture has taken place and

229 has caused cell coalescence. In addition, the periphery of the foams is denser for 2 and 5 wt.%

230 Mg addition, which reflects the pronounced collapse of cells taking place on the foam surface

231 during solidification.

232



233

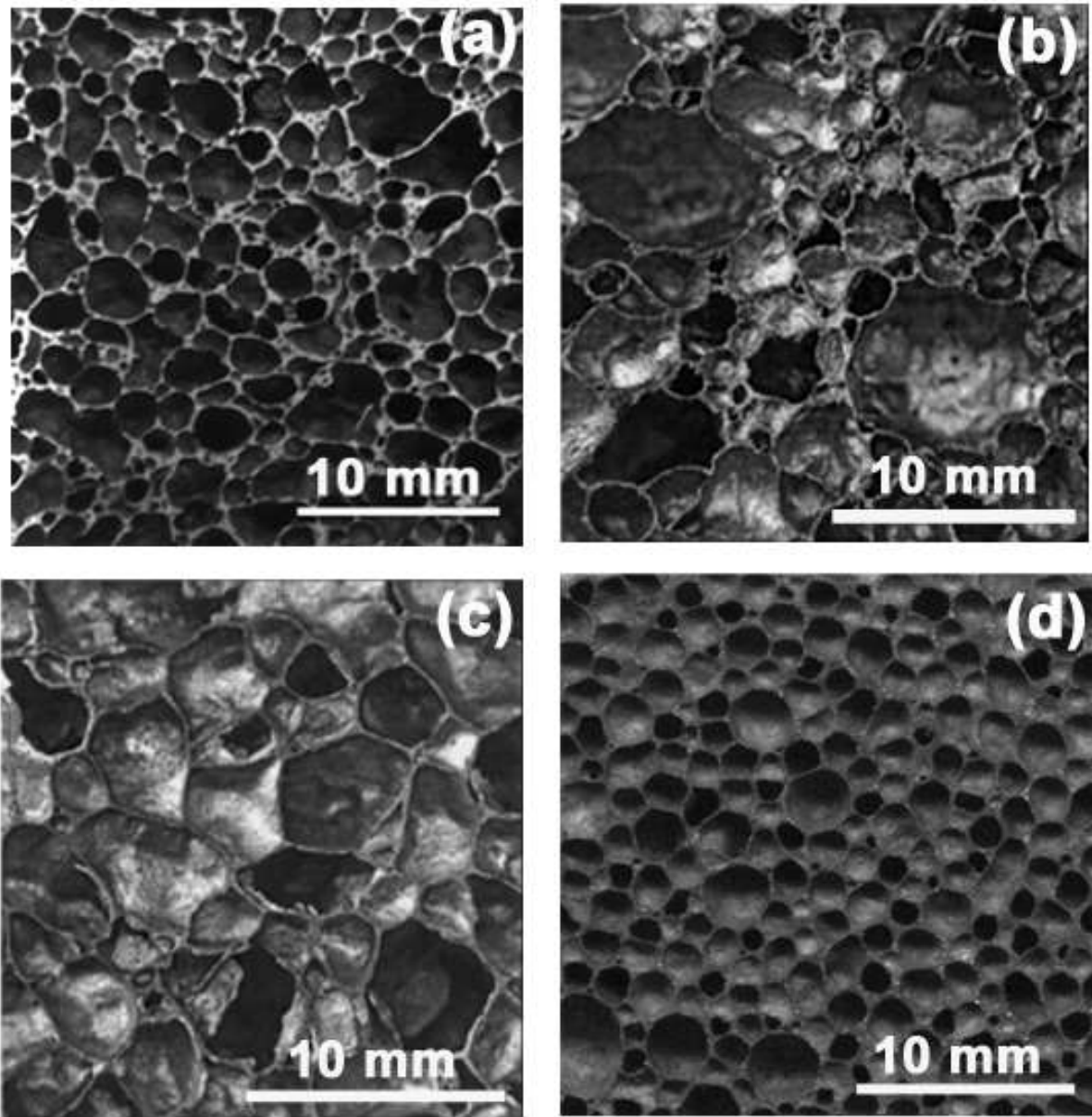
234

235 **Fig.9**X-ray tomographic reconstructions of transverse sections of re-melted Al scrap alloy
 236 foams produced by uninterrupted foaming in an alumina crucible at 973 K (700 °C). (a)
 237 0.13 wt.% Mg held for 100 s, (b) 1 wt.% Mg addition, (c) 2 wt.% Mg addition, (d) 5
 238 wt.% Mg addition, (b-d) held for 140 s. Arrows point at remnants of broken cell walls.

239 The foams containing 1 wt.% Mg excess obtained by foaming for 100 s and 140 s were cho-
 240 sen for a compressibility and energy absorption study due to their stability and uniform cell
 241 structure even after longer holding. Foams with 2 and 5 wt.% Mg excess possess more bro-
 242 ken cell walls and are therefore not taken for mechanical property evaluation. For the com-
 243 pression studies, 5 samples were sliced into cubes of (25×25) mm² size from the top to the

244 bottom of both foams that we call *foam-1* and *foam-2* depending on whether they were held for
245 100 s or 140 s, respectively. The densities of each sample obtained in this way vary from 0.19
246 to 0.37 g cm^{-1} (table 2). Figure 10a presents a closer view of the cross sections of a re-melted
247 Al scrap foam containing 1 wt.% Mg excess, foamed for 140s and having a density of
248 0.19 g cm^{-1} (*foam-2*). It is apparent that the cell structure is reasonably uniform.

249 Figures 10 b,c show the structures for Cymat and Alporas foams with densities of 0.38 g cm^{-1}
250 and 0.22 g cm^{-1} , respectively[14]. Figure 10d presents the structure of a Formgrip foam with a
251 density of 0.30 g cm^{-1} [15]. Although the foam densities are not comparable in this image, a
252 fair comparison of the foam structures can be made. It is well known that Cymat foams dis-
253 play a much wider distribution of cell sizes than Alporas foams. If foams with similar densi-
254 ties are compared (all at roughly 0.2 g cm^{-1}) then the Cymat foam is coarser with cells of a
255 mean diameter of roughly 7–8 mm [14], compared to 3–4 mm for Alporas[14, 16-17]. The
256 cell size and uniformity for the foam made from re-melted Al scrap are unlike those for the
257 Cymat foam (made by bubbling gas into an Al-Si melt using SiC particles to stabilise the
258 bubbles) and more closely resemble those for Alporas[18] and Formgrip foams [15], which are
259 also made by TiH_2 decomposition in a Al alloy melt.



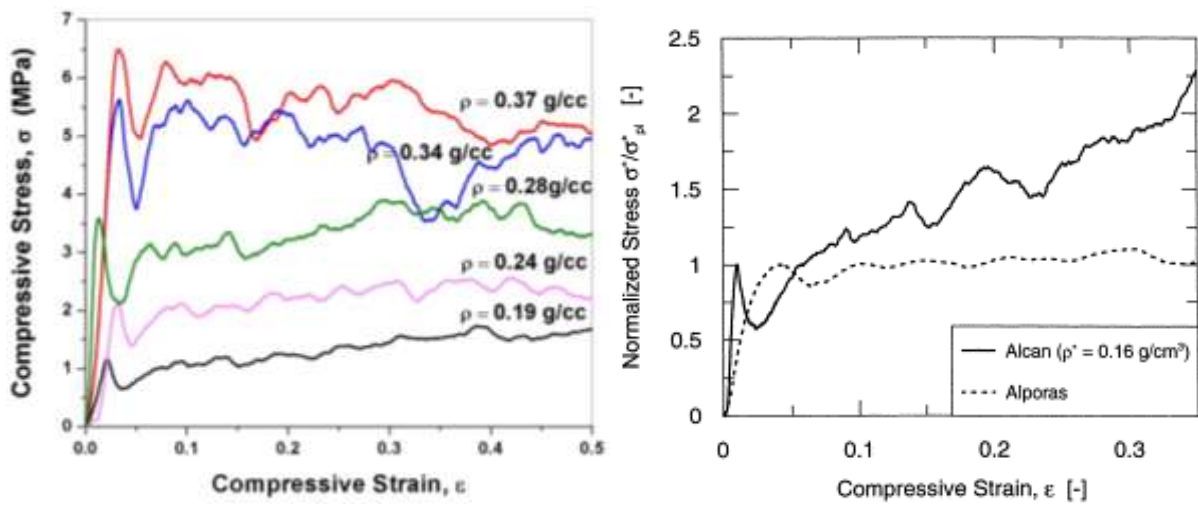
260

261 **Fig.10** Foam macrostructures for (a) foam made from re-melted scrap, *foam2* (1 wt.% Mg
 262 addition, holding time is 140s and density is $0.19 \text{ g}\cdot\text{cm}^{-1}$), (b) Cymat foam [3] (density
 263 = $0.38 \text{ g}\cdot\text{cm}^{-1}$), (c) Alporas foam [3] (density = $0.22 \text{ g}\cdot\text{cm}^{-1}$) and,(d) Formgrip foam
 264 (density = $0.3 \text{ g}\cdot\text{cm}^{-1}$) [4].

265 The compressive stress-strain curves for the re-melted Al scrap foams are given in Fig. 11a.
 266 As expected, there is an increase in the yield stress with increasing foam density. **Table 2**
 267 presents these values as measured from the initial maximum. Beyond yielding, the stress-
 268 strain curves undulate (the load rises and then drops sharply). These events are coupled with

269 observations during compressive testing of brittle fracture of the cell walls after collapse and
270 significant crumbling (images not shown).

271 **Table 2** also presents data for the energy absorbed per unit volume (in $\text{MJ}\cdot\text{m}^{-3}$) at 50% strain.
272 The efficiency of energy absorption across the range of densities is roughly 80–85%. For this
273 level of compressive strain, which is below the onset of densification (at typically 65–70%
274 strain), the flat plateau for the Alporas foam means that the efficiency is $>90\%$. For the Cy-
275 mat foam, it is $<70\%$ owing to the steadily increasing stress with strain[14, 19], see Fig.11b.



276

277 **Fig.11** Compressive stress–strain plots of (a) re-melted scrap alloy foams containing 1 wt.%
278 Mg excess obtained after 100 s and 140 s holding (b) Cymat (Alcan) foam and Alporas
279 foam (taken from [17]).

280 4. Discussion

281 The amount of oxide present in the alloy is 0.11 ± 0.01 wt.% based on the oxygen content in
282 the swarfs (machining chips and turnings). No heat treatment was carried out to increase the
283 oxygen content in the swarfs as it was done in previous studies [11-12]. If all the oxygen is
284 converted into oxide, this corresponds to 0.23 wt.% Al_2O_3 . After melting the swarfs, the con-
285 centration of oxides in the alloy would certainly increase during prolonged holding of the
286 swarfs (loose chips and turnings) at high temperature. The oxide content measured in the re-

287 melted scrap alloy is < 1 wt.%. Magnesium added to the melt for conditioning reacts with
288 aluminium oxide and forms $MgAl_2O_4$ (spinel) and MgO as already small amounts of Mg
289 (0.02 wt.%) can destabilize Al_2O_3 to form $MgAl_2O_4$ spinel. At higher Mg concentrations
290 (0.06 wt.%), MgO is formed at temperatures around 1000 K (727 °C)[20]. All the Mg concen-
291 trations studied here, namely 0.13% wt.% and excesses of 1, 2 and 5 wt.%, led to the for-
292 mation of $MgAl_2O_4$ and MgO, but there is no significant increase in $MgAl_2O_4$ or MgO on
293 increasing the Mg concentration. This could be attributed to the large size of the oxide films.
294 Vinod-Kumar et al. have shown that complete reaction of Mg with the oxides to form large
295 volumes of $MgAl_2O_4$ requires a higher oxide concentration (e.g. 5 wt.% of SiO_2) and the ox-
296 ides should be finer in size (the mean size was 44 μm in that case)[7]. In the present work, the
297 reaction is incomplete due to large oxides and therefore the excess Mg reacts with Si
298 (10.59 wt.% content in the alloy) to form Mg_2Si during solidification. Therefore, adding more
299 than 1 wt.% Mg during conditioning of the melt is not useful in fragmenting the oxide films
300 or distributing them in the matrix to a greater extent.

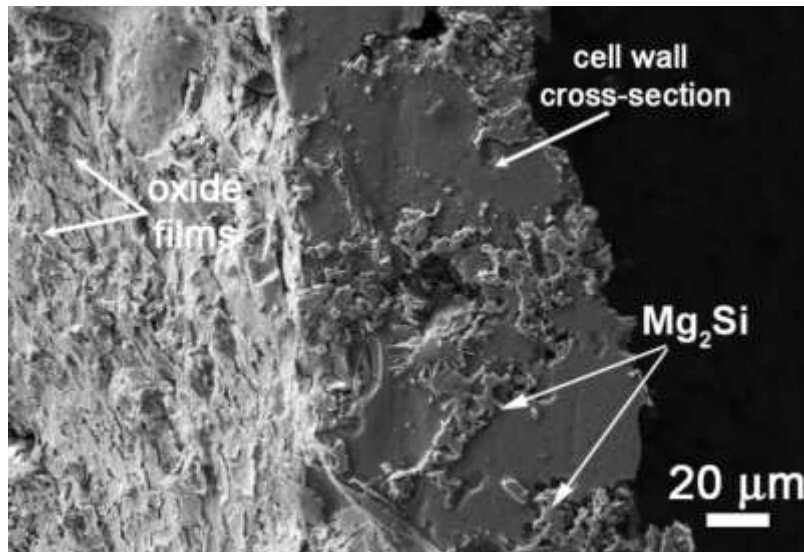
301 The uniform and equiaxed cell structure and good expansion of re-melted Al scrap alloy foam
302 without the addition of excess Mg (Fig. 4a, content only 0.13 wt.% Mg) indicates that long
303 oxide filaments can act as a stabilizing agent but only for a shorter period (~100 s). Holding
304 the liquid foam for 140 s caused collapse in the cells due to drainage, see Fig. 4b. Fragmenta-
305 tion of long oxide filaments into short films and their distribution in the matrix has significant
306 impact on the foaming behaviour particularly on expansion and stability upon longer holding.
307 The equally distributed cell structure as we could see in the foam containing 1 wt.% Mg (Fig.
308 5a) may be attributed to the fragmentation of long oxide filaments into shorter oxide films
309 and good wetting aided by $MgAl_2O_4$ particles.

310 Shape irregularities, i.e. non-equiaxed cells, are found frequently for foams containing 2 or
311 5 wt.% Mg excess. Even foams with 1 wt.% Mg show more non-equiaxed cells (based on the

312 mean circularity values shown in Fig. 8) in comparison to the foam with 0.13 wt.% Mg, but
313 not as significantly as for 2 and 5 wt.%. Assumptions were made that the increase in the vis-
314 cosity of melt (containing free Mg) during stirring and admixing the blowing agent[21]could
315 be a reason for the formation of a non-equiaxed cell structure. Incidentally, Alporas foams
316 that are made from a highly viscous melt produced by admixing Ca and stirring for as long as
317 15 to 20 min[18]exhibit an equiaxed cell structure. Therefore, the non-equiaxed cell structure
318 here should be rather attributed to the rupture of cell walls during solidification. Even during
319 solidification the phenomenon of solidification expansion (SE) [22] can occur, which leads to
320 cell wall thinning due to stretching and consecutive rupture and coalescence. This is clearly
321 evident from the remnants of broken cell wall observed in the 2D radiosopic images of
322 foams (Fig. 9a-d). Mukherjee et al. have pointed out that partially broken cell walls are a
323 clear indication that rupture took place during solidification[22]. If rupture occurred in the
324 liquid state the liquid metal in a broken film would be redistributed into the surrounding
325 structure and the geometry would be re-adjusted to an equiaxed bubble without leaving any
326 traces of the ruptured cell wall. During solidification, the increase in viscosity (caused by the
327 increasing solid fraction) will not allow the melt to redistribute in the cell wall and attain
328 equilibrium structure. The base alloy composition of the re-melted scrap investigated here is
329 Al-10 wt.% Si and has a larger solid-liquid co-existence region than in the base material of
330 Alporas foams that is almost pure Al.

331 However, non-equiaxed cells are seen more frequently in foams with higher Mg addition(1, 2
332 and 5 wt.%) than in the foam based on an alloy with just 0.13 wt.% Mg where cells are equi-
333 axed and fewer broken cell walls are observed. This indicates that the viscosity increase dur-
334 ing solidification is not only because of the increasing solid fraction but also due to the for-
335 mation of Mg_2Si particles. Mg_2Si forms at higher concentration of Mg and its volume frac-

336 tion increases with Mg concentration in the alloy (Fig. 3). Mg_2Si particles are large and
337 blocky in shape as seen in the interior of a foam cell wall (Fig. 12).



338

339 **Fig.12** SEM micrograph of re-melted Al scrap foam containing 2wt.%Mg excess showing
340 Mg_2Si phases in the interior of a cell wall and oxide films at the gas solid interface.

341 The compressive stress-strains plot of re-melted aluminium alloy scrap foams of various den-
342 sities containing 1 wt.% Mg excess show good strength but wavy strain plateaus, which
343 points at brittleness of the foams. This brittle behaviour is to be expected as the base alloy
344 (LM26) has very limited ductility (<1%) and this will decrease further with the presence of
345 significant levels of oxide films resulting from re-melting the scrap chips.

346 Comparisons can be made with the stress-strain behavior of commercial foams [17] which
347 have been normalized with respect to the initial maximum stress (Fig. 11b). At first inspec-
348 tion, the undulating curves resemble that for Cymat foam in which the cell material is also
349 brittle in nature (due to using a brittle Al-Si-SiC matrix alloy). However, unlike the Cymat
350 foam, the stress does not continually rise with progressive strain and in this respect there is
351 similarity to the Alporas foam. The much flatter stress-strain curve for the Alporas foam is
352 attributed to the much more uniform density and pore structure [17], which facilitates for-

353 mation of multiple deformation bands that are uniformly distributed throughout the sample
354 and enables progressive collapse to occur both by the expansion of existing bands and the
355 formation of new ones. In contrast, deformation of the more irregular Cymat foam is highly
356 localized in bands (generally containing large pores or areas of low density), which then pro-
357 gress to other regions in the foam only after the cells in the band have reached the point of
358 densification.

359 The initial maximum yield strengths for Alporas foams with densities in the range of 0.2–
360 0.4 g cm⁻¹ typically vary between 1.4–2.4 MPa [14,16,19]. For Cymat foams, the comparable
361 property is sensitive to the foaming direction and the gravity vector. For a comparable direc-
362 tion to that tested in this work, strengths between 1.2–5.0 MPa were observed[16]. The
363 strengths for the scrap and Cymat foams are of course higher than that for the Alporas foam
364 due to the higher inherent strength of the matrix material which is estimated to be 120–
365 170 MPa for Alporas, 310–390 MPa for Cymat[14,17] and 290–310 MPa for the foamable
366 re-melted scrap alloy (calculated as part of this study from hardness measurements of the
367 foamable base material containing 1 wt.% Mg).

368 Predictions for the yield strength using either the approach of Ref.[14] or [16] and typical
369 matrix strength data as given above reveal higher “knockdown” factors (i.e. deviations from
370 the predicted properties) for the Cymat foam than for either the Alporas or scrap-based
371 equivalents. This supports prior hypotheses that relate these larger reductions in the expected
372 strength (and indeed the stiffness) observed in the Cymat foam to the greater anisotropy, het-
373 erogeneity and variations in density as well as a higher occurrence and severity of cell wall
374 defects (wiggles, holes, fractures), which result from both the foaming and foam handling
375 processes specific to Cymat foam [14,16].

376

377 **5. Conclusions**

- 378 • Mg additions in excess to the level contained in the base scrap alloy (0.13 wt.%) promote
379 fragmentation and good distribution of oxides in the aluminium matrix. Formation of
380 MgAl_2O_4 (spinel) of octahedral morphology on the surface of the oxides can be observed.
381 Increasing Mg additions to 2 or 5 wt.% does not cause any notable further increase in the
382 formation of MgAl_2O_4 or MgO compared to 1 wt.% addition and no further fragmentation
383 of oxides or better distribution could be seen. However, an increase of Mg addition causes
384 the formation of Mg_2Si during solidification.
- 385 • Foaming re-melted Al scrap alloy without any additional Mg in excess to the 0.13 wt.% in
386 the base alloy led to an equiaxed cell structure, indicating that long oxide filaments can act
387 as stabilizing agent, but only if the holding time was limited to 100 s. Upon longer holding
388 (e.g. 140 s), strong drainage in the foam set in and foam collapse was observed.
- 389 • With 1 wt.% Mg excess, the expansion and the stability of foam upon longer holding
390 (140 s) are good due to fragmentation and good distribution of oxides. The foam with
391 1 wt.% Mg excess showed very good cell structure and a uniform cell size distribution.
- 392 • Increasing Mg additions to 2 or 5 wt.% led to stability even after longer holding but the
393 expansion slowed down. Corresponding foams showed a less equiaxed cell structure caused
394 by cell wall rupture and coalescence that occurred during solidification than foams without
395 or with just 1 wt.% Mg addition.
- 396 • Solidification expansion and the increase in viscosity during solidification of afoam are the
397 reason for non-equiaxed cell structures. In foams that contain 2 or 5 wt.% Mg excess, the
398 increase in viscosity during solidification and the formation of non-equiaxed cells are still
399 more pronounced due to the formation of Mg_2Si during solidification.
- 400 • During compression tests, foams with 1 wt.% Mg excess (having optimum cell structure) of
401 various densities exhibit brittle crumbling of the cell walls. This is the typical compressive

402 behaviour of a low-ductility Al-Si casting alloy containing significant levels of oxides.
403 However, their uniform pore structure leads them to have flatter compression stress plat-
404 eaus, higher energy absorption efficiencies and a reduced “knockdown” in properties,
405 which is comparable with that of Alporas foams made in the same way. Therefore, foams
406 made from re-melted alloy scrap could offer the same performance as Alporas foams but at
407 a lower cost.

408 **Acknowledgements**

409 The corresponding author thanks German DFG, Grants GA 1304/2-1 and BA 1170/17-1 and
410 Indian Naval Research Board, Grants NRB-317/MAT/13-14 for the support of this study
411

412 **References**

- 413 1. J. Banhart, Prog. Mater. Sci., 2001. vol. 46, pp. 559-632.
- 414 2. L. Drenchev, J. Sobczak, S. Malinov, W. Sha, Mater.Sci. Technol., 2006, vol. 22, pp.
415 1135-47.
- 416 3. S. W. Ip, S.Y.Wang, J. M. Toguri, Can. Metall. Q, 1999, vol. 38, pp. 81-92.
- 417 4. J. Banhart, J.Met., 2000, vol.52,pp. 22-27.
- 418 5. N. Babcsán, D. Leitlmeier, H.P. Degischer, Materialwiss.Werkstofftech., 2003, vol.34,
419 pp. 22-29.
- 420 6. N. Babcsán, F.Garcia-Moreno, J. Banhart, Colloids Surf., A, 2007,vol.309, pp. 254-63.
- 421 7. G. S. Vinod Kumar, M. Chakraborty, F. Garcia-Moreno, J. Banhart, Metall. Mater.
422 Trans. A, 2011, vol.42, pp. 2898-908.
- 423 8. J. Banhart, Adv. Eng. Mater., 2006,vol.8, pp.781-94.
- 424 9. W. Ha, S. K. Kim, H.H Jo, Y.J Kim, Mater.Sci.Technol., 2005, vol.21, pp. 495-99.
- 425 10. M. Haesche, D. Lehnhus, J. Weise, M. Wichmann, I. C. M.Mocellin, J. Mater.Sci.
426 Technol.,2010, vol.26, pp. 845-50.

- 427 11. G. S. Vinod Kumar, K. Heim, F. Garcia-Moreno, J. Banhart, A. R. Kennedy, Adv.
428 Eng. Mater., 2013, vol.15, pp.129-33.
- 429 12. G. S. Vinod Kumar, K. Heim, F. Garcia-Moreno, J. Banhart, A. R. Kennedy, Int. J.
430 Mater. Res., 2015, vol.106, pp. 978-87.
- 431 13. M. Mukherjee, U. Ramamurty, F. Garcia-Moreno, J. Banhart, Acta Mater., 2010,
432 vol.58, pp. 5031-42.
- 433 14. E. Andrews, W. Sanders, L.J. Gibson, Mater. Sci. Eng. A, 1999, vol.270, pp. 113-24.
- 434 15. V. Gergely and B. Clyne, Adv. Eng. Mater., 2000, vol.2, pp.175-78.
- 435 16. O.Olurin, N. Fleck, M. Ashby, Mater. Sci. Eng. A, 2000, vol.291, pp.136-46.
- 436 17. A. E. Simone and L.J. Gibson, Acta Mater., 1998. vol.46, pp.3109-23.
- 437 18. T. Miyoshi, M. Itoh, S. Akiyama, A. Kitahara, Adv. Eng. Mater., 2000, vol.2, pp.
438 179-83.
- 439 19. U. Ramamurty, A. Paul, Acta Mater., 2004, vol.52, pp.869-76.
- 440 20. B.C. Pai, G. Ramani, R. M. Pillai, K. G. Satyanarayana, J.Mater.Sci., 1995, vol.30, pp.
441 1903-11.
- 442 21. S.Y. Kim, Y.S. Um, B.Y. Hur, Mater. Sci. Forum, 2006, vol. 510-511, pp. 902-5, 2006
- 443 22. M. Mukherjee, F. Garcia-Moreno, J. Banhart, Scripta Mater., 2010, vol.63, pp. 235-38.
- 444
- 445
- 446
- 447
- 448
- 449
- 450

451 **Table Caption**

452 **Table 1. Chemical composition of swarf chips measured by OES**

Element	Si	Cu	Fe	Mn	Mg	Zn	Al
wt.%	10.50	1.60	1.20	0.29	0.13	1.10	balance

453

454 **Table 2. Mechanical properties for scrap foams**

Foams	Mg added in excess to 0.13 wt.% (wt.%)	Holding time (s)	density (g·cm⁻¹)	yield strength (MPa)	E_{abs}(MJ·m⁻³)
<i>foam 1</i>	1	100s	0.34	5.63	2.36
			0.37	6.49	2.64
<i>foam 2</i>	1	140s	0.19	1.16	0.64
			0.24	2.10	1.07
			0.28	3.58	1.47

455

456